Journal of Medicinal Chemistry

Article

pubs.acs.org/jmc

Synthesis and Evaluation of Novel Radioligands for Positron Emission Tomography Imaging of Metabotropic Glutamate Receptor Subtype 1 (mGluR1) in Rodent Brain

Masayuki Fujinaga,[†,∥] Tomoteru Yamasaki,[†,‡,∥] Joji Yui,[†] Akiko Hatori,[†] Lin Xie,[†] Kazunori Kawamura,[†] Chiharu Asagawa,[†] Katsushi Kumata,[†] Yuichiro Yoshida,[†,§] Masanao Ogawa,[†,§] Nobuki Nengaki,[†,§] Toshimitsu Fukumura,[†] and Ming-Rong Zhang*[,†]

[†]Molecular Imaging Center, National Institute of Radiological Sciences, 4-9-1 Anagawa, Inage-ku, Chiba 263-8555, Japan

[‡]Graduate School of Pharmaceutical Sciences, Tohoku University, Aoba-ku, Sendai 980-8574, Japan

[§]SHI Accelerator Service Co. Ltd., 5-9-11 Kitashinagawa, Shinagawa-ku, Tokyo 141-8686, Japan

Supporting Information

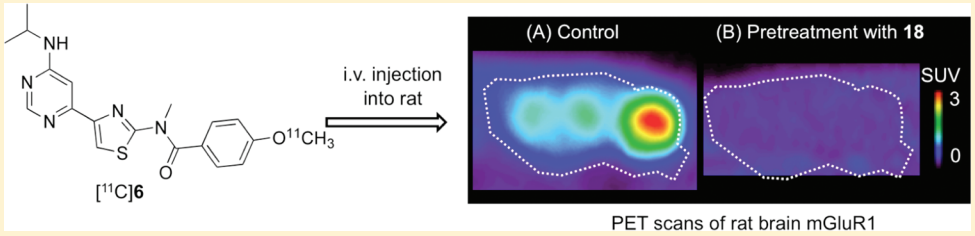

PET scans of rat brain mGluR1

ABSTRACT: We designed three novel positron emission tomography ligands, *N*-(4-(6-(isopropylamino)pyrimidin-4-yl)-1,3-thiazol-2-yl)-4-[^{11}C]methoxy-*N*-methylbenzamide ([^{11}C]**6**), 4-[^{18}F]fluoroethoxy-*N*-[4-[6-(isopropylamino)pyrimidin-4-yl]-1,3-thiazol-2-yl]-*N*-methylbenzamide ([^{18}F]**7**), and 4-[^{18}F]fluoropropoxy-*N*-[4-[6-(isopropylamino)pyrimidin-4-yl]-1,3-thiazol-2-yl]-*N*-methylbenzamide ([^{18}F]**8**), for imaging metabotropic glutamate receptor type 1 (mGluR1) in rodent brain. Unlabeled compound **6** was synthesized by benzoylation of 4-pyrimidinyl-2-methylaminothiazole **10**, followed by reaction with isopropylamine. Removal of the methyl group in **6** gave phenol precursor **12** for radiosynthesis. Two fluoroalkoxy analogues **7** and **8** were prepared by reacting **12** with tosylates **13** and **14**. Radioligands [^{11}C]**6**, [^{18}F]**7**, and [^{18}F]**8** were synthesized by *O*-[^{11}C]methylation or [^{18}F]fluoroalkylation of **12**. Compound **6** showed high in vitro binding affinity for mGluR1, whereas **7** and **8** had weak affinity. Autoradiography using rat brain sections showed that [^{11}C]**6** binding is aligned with the reported distribution of mGluR1 with high specific binding in the cerebellum and thalamus. PET study with [^{11}C]**6** in rats showed high brain uptake and a similar distribution pattern to that in autoradiography, indicating the usefulness of [^{11}C]**6** for imaging brain mGluR1.

INTRODUCTION

Glutamate is an excitatory neurotransmitter in the central nervous system (CNS) and is involved in many pathological conditions of CNS. Glutamate receptors were divided into metabotropic (mGluRs) and iontropic types based on their biological functions and molecular structures. MGluRs were classified into three groups including eight subtypes according to sequence homology, coupling mechanisms to G-protein, and pharmacological activity.[1,2] Group I mGluRs (mGluR1 and mGluR5) play important physiological roles in regulating ion channels and synaptic transmission, and in synaptic plasticity, which underlies memory and learning.[3−5] It has been reported that mGluR1 may be a drug target for the treatment of diseases such as stroke, epilepsy, pain, cerebellar ataxia, Parkinson's disease, anxiety, and mood disorders.[6−10]

Positron emission tomography (PET) with radioligands is a molecular imaging technique that enables study of the living human brain and in particular of specific proteins involved in pathophysiology or as targets for therapeutic interventions. Although many PET probes have been developed for various targets, such as enzymes, transporters, plaques, ion channels, and receptors, some important molecular targets, including mGluR1, still lack useful radioligands for clinical study. PET with a specific mGluR1 ligand could be an important tool for understanding the role of this receptor in health and disorders in which mGluR1 is involved and also for the development of new drugs targeting this receptor.

The distribution of mGluR1 in the brain has been studied using in vitro autoradiography and histologic analysis.[11,12] Studies showed a wide distribution of mGluR1 in brains with, for example, a high level in the cerebellum, moderate or low level in the thalamus, striatum, and cerebral cortex, and a very low level in the brain stem. Intense efforts have been made over recent years to develop PET ligands for imaging brain mGluR1. Examples include [^{11}C]JNJ-16567083 ([^{11}C]**1**),[13] [^{11}C]YM-202074

Received: November 25, 2011
Published: February 8, 2012

   dx.doi.org/10.1021/jm201590g | J. Med. Chem. 2012, 55, 2342−2352

Scheme 1. Chemical Structures of PET Ligands for mGluR1

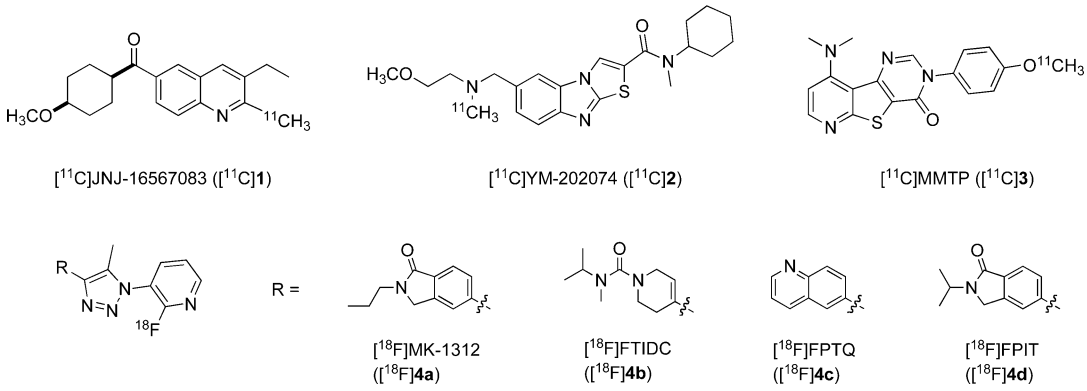

([^{11}C]**2**),[14] [^{11}C]MMTP ([^{11}C]**3**),[15] [^{18}F]MK-1312 ([^{18}F]**4a**),[16] [^{18}F]FTIDC ([^{18}F]**4b**),[17] [^{18}F]FPTQ ([^{18}F]**4c**),[18] and [^{18}F]FPIT ([^{18}F]**4d**)[19] (Scheme 1). These radioligands had high in vitro binding affinity for mGluR1, but their in vivo binding for mGluR1 visualized in the brain with PET was much lower than the corresponding in vitro binding. Moreover, in vivo binding for mGluR1 was only seen in the cerebellum.[13,15,18] No imaging study of mGluR1 in the human brain has been performed for clinical usefulness.

Recently, when searching for a pharmacophore different from the chemical structures reported, we developed 4-[^{18}F]fluoro-*N*-[4-(6-(isopropylamino)pyrimidin-4-yl)-1,3-thiazol-2-yl]-*N*-methylbenzamide ([^{18}F]**5**, Scheme 2) as a novel

Scheme 2. Chemical Structure of 5−8 and Their Labeled Compounds

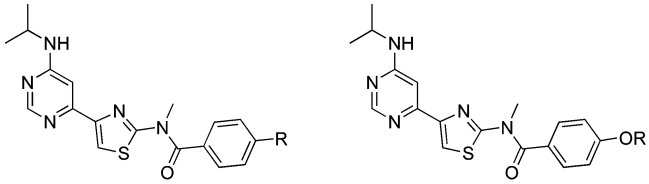

PET ligand for imaging brain mGluR1.[20,21] PET with [^{18}F]**5** showed significant signals in rat and monkey brain regions, not only an mGluR1-rich cerebellum but also mGluR1-moderate or low regions, such as the thalamus, striatum, and cerebral cortex.[21] The uptake ratio of radioactivity, an index reflecting the in vivo specific binding of [^{18}F]**5** to mGluR1, between the cerebellum and mGluR1-negligible pons in the rat brain reached approximately 10, which was the highest among all reported PET ligands for this receptor. Currently, [^{18}F]**5** is being prepared for clinical imaging study of brain mGluR1 in our facility.

The objective of this study was to develop new ^{11}C or ^{18}F-labeled PET ligands with high in vitro binding affinity, in vitro and in vivo specific binding for mGluR1, and with improved kinetics over [^{18}F]**5** to quantitatively determine mGluR1 in the brain. A disadvantage of [^{18}F]**5** is slow kinetics in the rat and monkey brains.[21] After injection of [^{18}F]**5** into rats, uptake of radioactivity increased in all brain regions during a PET scan, which may create complication in quantitative analysis for measuring mGluR1 density with PET. On the other hand, [^{18}F]**5** was prepared by heating a nitro precursor with [^{18}F]F^- at 180 °C, at which the nitro precursor was easily decomposed.[20] Separation of [^{18}F]**5** with from the nitro precursor and by-product with high-performance liquid chromatography (HPLC) required more than 20 min.

In this study, using [^{18}F]**5** as a lead compound, we designed three novel radioligands [^{11}C]**6**, [^{18}F]**7**, and [^{18}F]**8** (Scheme 2) and evaluated their potentials as PET ligands for mGluR1. As shown in their chemical structures, a methoxy group was introduced into [^{11}C]**6** instead of a fluorine atom in [^{18}F]**5**. It is easy to label **6** using [^{11}C]methyl iodide with two levels of specific activity (37−185 GBq/μmol[22] and 3700−7400 GBq/μmol[23]) available in our institute. Further, using the same phenol precursor, we synthesized two [^{18}F]fluoroalkoxy analogues [^{18}F]**7** and [^{18}F]**8** and characterized their specific binding for mGluR1 in the brain.

Here, we report (1) chemical synthesis, (2) radiolabeling, (3) in vitro binding affinity and autoradiography, and (4) small-animal PET studies of a small set of PET mGluR1 radioligands.

RESULTS AND DISCUSSION

Chemistry. The novel unlabeled compounds **6**−**8** were synthesized according to reaction sequences delineated in Scheme 3. Ethoxyvinylpyrimidine **9** was synthesized by coupling 4,6-dichloropyrimidine with tributyl(1-ethoxyvinyl)-stannane in the presence of tetrakis(triphenylphosphine)-palladium (0) ($Pd(PPh_3)_4$). Reaction of **9** with *N*-bromosuccinimide, followed by treatment with *N*-methylthiourea, gave 4-(6-chloropyrimidin-4-yl)-*N*-methylthiazol-2-amine (**10**).[24] Benzoylation of **10** with 4-methoxybenzoyl chloride afforded **11**, which was heated with isopropylamine to give **6** in 19% total yield from 4,6-dichloropyrimidine. Removal of the methyl group in **6** with boron tribromide (BBr_3) gave the desmethyl phenol precursor **12** used for the present radiosyntheses. To prevent contamination by a trace amount of **6**, which would decrease the specific activity of [^{11}C]**6**, precursor **12** prepared by the desmethylation was further purified by semipreparative HPLC (Supporting Information Figure 1).

Two fluoroalkoxy analogues **7** and **8** were synthesized by heating precursor **12** with tosylates **13** and **14**, which were obtained by the reaction of fluoroalcohol with 4-methylbenzenesulfonyl chloride[25] in the presence of K_2CO_3 at 70 °C for 6 h in 52% and 60% yields, respectively.

dx.doi.org/10.1021/jm201590g | J. Med. Chem. 2012, 55, 2342−2352

Scheme 3. Syntheses of 6−8 and Precursor 12[a]

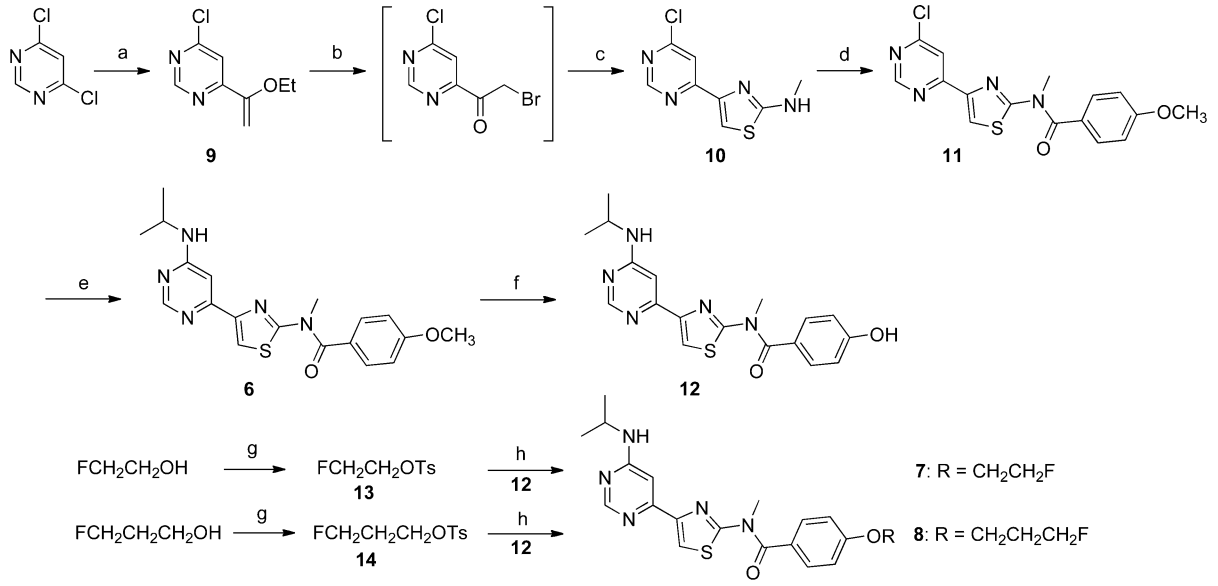

[a]Reagents and conditions: (a) ethyl 1-(tributylstannyl)vinyl ether, $Pd(PPh_3)_4$, DMF, 80 °C, 5 h; (b) THF, H_2O, 1-bromopyrrolidine-2,5-dione, room temperature, 2 h; (c) *N*-methylthiourea, room temperature, 2 h; (d) 4-methoxybenzoyl chloride, Et_3N, toluene, 100 °C, 10 h; (e) isopropylamine, K_2CO_3, 1,4-dioxane, 80 °C, 16 h; (f) BBr_3, CH_2Cl_2, −40 °C, then room temperature, overnight; (g) *p*-toluenesulfonyl chloride, pyridine, CH_2Cl_2, room temperature, 24 h; (h) K_2CO_3, DMF, 70 °C, 6 h.

Scheme 4. Radiosyntheses of [^{11}C]6, [^{18}F]7, and [^{18}F]8[a]

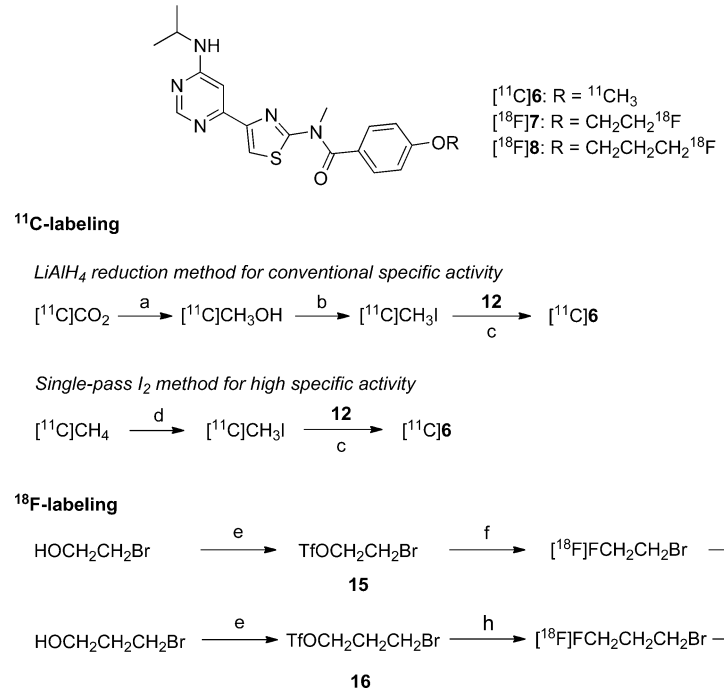

[a]Reagents and conditions: (a) $LiAlH_4$, THF, −15 °C, 2 min; (b) hydroiodic acid, 180 °C, 2 min; (c) DMF, NaOH, 70 °C, 5 min; (d) I_2, 630 °C; (e) trifluoromethanesulfonic anhydride, 2,6-lutidine, CH_2Cl_2, 0 °C, 1 h; (f) [^{18}F]KF, Kryptofix 222, 1,2-dichlorobenzene, 130 °C, 2 min; (g) NaOH, DMF, 90 °C, 10 min; (h) [^{18}F]KF, Kryptofix 222, 1,2-dichlorobenzene, 180 °C, 2 min; (i) NaOH, DMF, 120 °C, 10 min.

Radiosynthesis of [^{11}C]**6**, [^{18}F]**7**, and [^{18}F]**8** was performed using a homemade automated synthesis system. This system is equipped with two units for [^{11}C]methylation and [^{18}F]-fluoroalkylation routinely used in our facility.[26]

The *O*-[^{11}C]methyl ligand [^{11}C]**6** was prepared by reacting precursor **12** with [^{11}C]methyl iodide ([^{11}C]MeI) of two levels of specific activity (Scheme 4). As for the conventional specific activity (37−185 GBq/μmol), [^{11}C]MeI for radiolabeling was prepared by reducing cyclotron-produced [^{11}C]carbon dioxide ([^{11}C]CO_2) with lithium aluminum hydride ($LiAlH_4$), followed by iodination with 57% hydroiodic acid.[22] After distillation and drying, [^{11}C]MeI was transferred into a DMF solution of **12** and NaOH. The [^{11}C]methylation proceeded efficiently for 5 min at 70 °C. Semipreparative HPLC purification for the

dx.doi.org/10.1021/jm201590g | J. Med. Chem. 2012, 55, 2342−2352

Table 1. Lipophilicity and In Vitro Binding Affinity

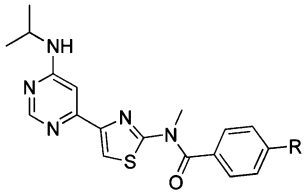

				in vitro binding affinity (nM)[c]		
		lipophilicity		mGluRl		mGluR5
compd	R	cLogD[a]	LogD[b]	IC_{50}	K_i	IC_{50}
6	OCH_3	2.64	2.57	32.7 ± 1.2	12.6 ± 1.2	>10000
7	OCH_2CH_2F	2.79	2.59	395.1 ± 1.2	152.7 ± 1.2	>10000
8	$OCH_2CH_2CH_2F$	3.15	2.80	>10000	>5000	>10000
5	F	2.35	1.45	13.9 ± 1.2[d]	5.4 ± 1.2	>10000

[a]cLogD values were calculated with Pallas 3.4 software. [b]LogD values were determined in the octanol/phosphate buffer (pH = 7.40) by the shaking flash method (n = 3; maximum range, ± 5%). [c]Values of in vitro binding affinity are the mean ± SE measured in duplicate brain homogenates. [d]Value of functional IC_{50} using CHO cells expressing human mGluRl was 5.1 ± 2.0 nM as reported in ref 24.

reaction mixtures gave [^{11}C]**6** with 22 ± 5% (n = 21) radiochemical yields (decay-corrected) based on [^{11}C]CO_2 (Supporting Information Figure 2). Starting from 15−20 GBq of [^{11}C]CO_2, 0.9−2.1 GBq of [^{11}C]**6** was produced with 25 ± 3 min (n = 21) of synthesis time from the end of bombardment (EOB). The specific activity of [^{11}C]**6** was 95−140 GBq/μmol at the end of synthesis (EOS).

As for the high specific activity, [^{11}C]**6** was prepared by reacting **12** with [^{11}C]MeI of 3700−7400 GBq/μmol. In our facility, several [^{11}C]methylated PET ligands high specific activity have been synthesized and used to visualize and assess receptors present at extremely low density or new binding sites in the brain.[23,27,28] For radiolabeling, [^{11}C]MeI was produced by iodination of [^{11}C]CH_4 formed in the target chamber in situ (the single pass I_2 method). After the [^{11}C]methylation reaction, [^{11}C]**6** was obtained with 6 ± 1% (n = 3) radiochemical yield (decay-corrected) based on [^{11}C]CH_4 (Supporting Information Figure 2). Starting from about 37 GBq of [^{11}C]CH_4, 0.9−1.1 GBq of [^{11}C]**6** was produced with 29 ± 1 min (n = 3) of synthesis time from EOB. The specific activity of [^{11}C]**6** was 4370−7840 GBq/μmol at EOS.

Two [^{18}F]fluoroalkoxy ligands [^{18}F]**7** and [^{18}F]**8** were synthesized by reacting **12** with 1-bromo-2-[^{18}F]fluoroethane ([^{18}F]FEtBr)[29] and 1-bromo-3-[^{18}F]fluoropropane ([^{18}F]-FPrBr), respectively (Scheme 4). The labeling agent [^{18}F]FEtBr or [^{18}F]FPrBr was prepared by the [^{18}F]fluorination of 2-bromoethyl trifluoromethanesulfonate (**15**) or 3-bromopropyl trifluoromethanesulfonate (**16**) with [^{18}F]F^- using a home-made synthetic unit.[30,31] After a solution of **15** or **16** in 1,2-dichlorobenzene was added to dried [^{18}F]F^-, the reaction mixture was immediately heated to produce [^{18}F]FEtBr or [^{18}F]FPrBr, which was distilled, dried, and trapped in a solution of **12** and NaOH in DMF. The purification of [^{18}F]FEtBr (boiling point: 71.5 °C) or [^{18}F]FPrBr (boiling point: 101 °C) by distillation was effective,[29] because this procedure can separate both reagents from their reaction mixtures to achieve radiochemical purity of >95% of [^{18}F]FEtBr or [^{18}F]FPrBr. After trapping each reagent, the [^{18}F]fluoroalkylation mixture was heated at 90 or 120 °C for 10 min. HPLC purification of the reaction mixtures gave [^{18}F]**7** and [^{18}F]**8** in 24 ± 2% (n = 3) and 2% radiochemical yields based on [^{18}F]F^- (Supporting Information Figure 2), corrected for physical decay in the synthesis times of 59 ± 5 and 58 min from EOB, respectively. Starting from 4.1−6.3 GBq of [^{18}F]F^-, 0.7−1.0 GBq of [^{18}F]**7**, and 55 MBq of [^{18}F]**8** was obtained with specific activity of 330−410 GBq/μmol at EOS. The [^{18}F]fluoropropylation efficiency for **12** was much lower than the [^{18}F]fluoroethylation efficiency, which was due to decrease in the inductive effect of fluorine atom with the prolonging of methylene chains in the two labeling agents.

The identity of [^{11}C]**6**, [^{18}F]**7**, and [^{18}F]**8** was confirmed by coinjection with the corresponding unlabeled **6**−**8** on reverse phased−analytical HPLC. In the final product solutions, their radiochemical purity was higher than 99% (Supporting Information Figure 3). No significant peak corresponding to the unreacted **12** was observed on any HPLC charts for the final products. Moreover, these radioligands did not show radiolysis at room temperature for 180 min after formulation, indicating their radiochemical stability with the time of at least one PET scan. The analytical results were in compliance with our in-house quality control/assurance specifications of radiopharmaceuticals.

Computation and Measurement of Ligand Lipophilicities. The computed values of lipophilicities at pH = 7.4 (cLogD) for [^{11}C]**6**, [^{18}F]**7**, and [^{18}F]**8** were 2.64−3.15 (Table 1). The values of lipophilicities (LogD) were 2.57−2.80 measured by the Shake Flask method.[17] The lipophilicity values of these radioligands are higher than that of [^{18}F]**5** (LogD, 1.45; cLogD, 2.35) and lie in the range normally considered favorable for a PET ligand.[32]

In Vitro Binding Assays. In vitro binding affinities (K_i) of **6**−**8** for mGluR1 were measured from competition against the binding of mGluR1-selective [^{18}F]**5** using rat brain homogenates. As shown in Table 1, **6** showed high binding affinity (K_i = 12.6 nM) for mGluR1, although the affinity was weaker than that of **5** (K_i = 5.4 nM). Higher electron density in the anisole ring in **6** than that in the fluorobenzene ring in **5** may be the main cause of the decrease in the binding affinity for mGluR1. Among these compounds, fluoropropyl **8** displayed the lowest affinity (K_i > 5 μM). This result suggested that the bulk-increasing group attached to the 4-position of the benzene ring may not fit the binding site on the mGluR1 domain, resulting in a significant decrease in the binding affinity of **8**.

On the other hand, the binding affinity of **6**−**8** for mGluR5 was measured from competition against the binding of mGluR5-selective [^{11}C]ABP688[33] ([^{11}C]**17**; Supporting Information

dx.doi.org/10.1021/jm201590g | J. Med. Chem. 2012, 55, 2342−2352

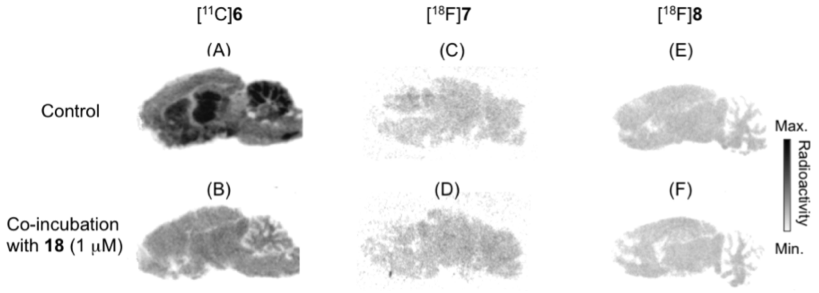

Figure 1. Representative in vitro autoradiographic images of rat brains with [^{11}C]**6** (9.2 MBq, 0.5 nmol, A,B), [^{18}F]**7** (0.4 MBq, 5 pmol, C,D), and [^{18}F]**8** (0.4 MBq, 4 pmol, E,F). (A) [^{11}C]**6** only; (B) [^{11}C]**6** with **18** (1 μM); (C) [^{18}F]**7** only; (D) [^{18}F]**7** with **18** (1 μM); (E) [^{18}F]**8** only; (F) [^{18}F]**8** with **18** (1 μM).

Table 2. Biodistribution (% ID/g Tissue: mean ± SE, n = 4) in Mice after Injection of [^{11}C]6

tissue	1 min	5 min	15 min	30 min	60 min
blood	3.79 ± 0.33	1.95 ± 0.03	0.96 ± 0.10	0.67 ± 0.03	0.64 ± 0.03
heart	4.63 ± 1.19	2.09 ± 0.12	1.19 ± 0.17	0.91 ± 0.05	0.81 ± 0.05
lung	5.17 ± 0.53	2.90 ± 0.16	1.91 ± 0.14	1.92 ± 0.13	1.57 ± 0.18
liver	8.16 ± 2.68	8.34 ± 0.61	5.57 ± 0.54	4.68 ± 0.22	3.97 ± 0.26
spleen	1.97 ± 0.44	1.96 ± 0.17	1.98 ± 0.23	2.14 ± 0.59	2.36 ± 0.56
kidney	8.67 ± 1.44	5.64 ± 0.33	3.78 ± 0.29	3.32 ± 0.21	2.92 ± 0.28
small intestine	3.65 ± 0.44	4.55 ± 0.32	4.98 ± 0.66	4.07 ± 0.44	3.97 ± 0.33
muscle	2.04 ± 0.07	1.22 ± 0.32	0.95 ± 0.15	0.64 ± 0.08	0.52 ± 0.11
testis	0.72 ± 0.15	0.83 ± 0.05	0.54 ± 0.06	0.38 ± 0.06	0.33 ± 0.10
brain	3.10 ± 0.34	3.21 ± 0.13	3.14 ± 0.20	2.38 ± 0.17	1.85 ± 025

Scheme 1) using the same homogenates of rat brain. As shown in Table 1, **6**–**8** did not show significant inhibitory effects (IC_{50} > 10 μM) on [^{11}C]**17** binding in the homogenate, indicating their weak binding affinities for mGluR5.

In Vitro Autoradiography. Figure 1 shows representative in vitro autoradiograms of [^{11}C]**6**, [^{18}F]**7**, and [^{18}F]**8** on sagittal sections of rat brains. As for [^{11}C]**6**, the distribution pattern of radioactivity was heterogeneous, with the highest level in the cerebellum (Figure 1A). Moderate radioactivity was seen in the thalamus and a low level was determined in the striatum. The lowest radioactivity was detected in the brain stem. This autoradiographic result was consistent with the distribution pattern of mGluR1 in the rat brain.[11] Co-incubation with mGluR1-selective JNJ-16259685[34] (**18**, Figure 1B; Supporting Information Scheme 1) reduced radioactivity in the sections to 30% of radioactivity in the control sections. The specific binding of [^{11}C]**6** for mGluR1 accounted for >70% of total binding in the brain, demonstrating high in vitro specificity of this radioligand for mGluR1.

Autoradiograms of [^{18}F]**7** (Figure 1C) and [^{18}F]**8** (Figure 1E) showed much lower radioactivity in the brain sections than that of [^{11}C]**6** (Figure 1A). The distribution of radioactivity was homogeneous among all brain regions. Further, coincubation with **18** (1D,F) did not affect radioactivity in the sections significantly. These results indicated that the two [^{18}F]fluoroalkoxy ligands had a weak signal of mGluR1 in the brain, which was consistent with their weak in vitro binding affinity with mGluR1 (Table 1).

On the basis of these in vitro results, we ceased to further evaluate [^{18}F]**7** and [^{18}F]**8**, and selected [^{11}C]**6** for in vivo evaluation.

Biodistribution Study. The distribution of radioactivity in mice was measured at designated experimental time points after injection of [^{11}C]**6** (Table 2). At 1 min after injection, high uptake (>3% injected dose per gram of wet tissue, % ID/g) appeared in the blood, heart, lung, liver, kidney, and small intestine. After the initial phage, the radioactivity levels in most tissues decreased, while that in the liver continually increased until 5 min and then decreased slowly. High uptake in the liver, kidney, and small intestine suggested that hepatobiliary and urinary excretion, as well as the intestinal reuptake pathway, might dominate the whole-body distribution of radioactivity and rapid washout from the body after injection of this radioligand.

On the other hand, high initial uptake was found in the mouse brain, the target tissue in this study, indicating that [^{11}C]**6** passes across the blood–brain barrier and enters the brain, which is a prerequisite for a favorable PET ligand used in brain imaging. The considerable brain uptake was consistent with the suitable lipophilicity (LogD = 2.57) of [^{11}C]**6**. At 30 min after the injection, brain uptake remained at >2% ID/g, suggesting that [^{11}C]**6** has some specific binding in the brain.

Small-Animal PET Studies on Rats. The in vivo uptake, kinetics, and specific binding in the rat brains were examined using small-animal PET with [^{11}C]**6** with conventional specific activity.

Figures 2A–L show representative PET images of rat brains after injection of [^{11}C]**6**. To confirm the corresponding brain regions, anatomical template MRI images of rat brains were used as shown in Figures 2M–P. Baseline PET showed high brain penetration and accumulation of radioactivity in the brain regions (Figure 2A–D). The highest uptake was seen in the cerebellum (Figure 2A,B), followed by the thalamus (Figure 2A,C) and striatum (Figure 2A,D). The lowest radioactivity was determined in the pons (Figure 2B). This distribution pattern of uptake reflected the distribution of mGluR1 in the brain, which was similar to the in vitro autoradiograms for [^{11}C]**6**. As shown in the time–activity curves (TACs) of brain regions (Figure 3A), radioactivity in the cerebellum gradually increased after injection, peaked at 45 min, and decreased to

dx.doi.org/10.1021/jm201590g | J. Med. Chem. 2012, 55, 2342–2352

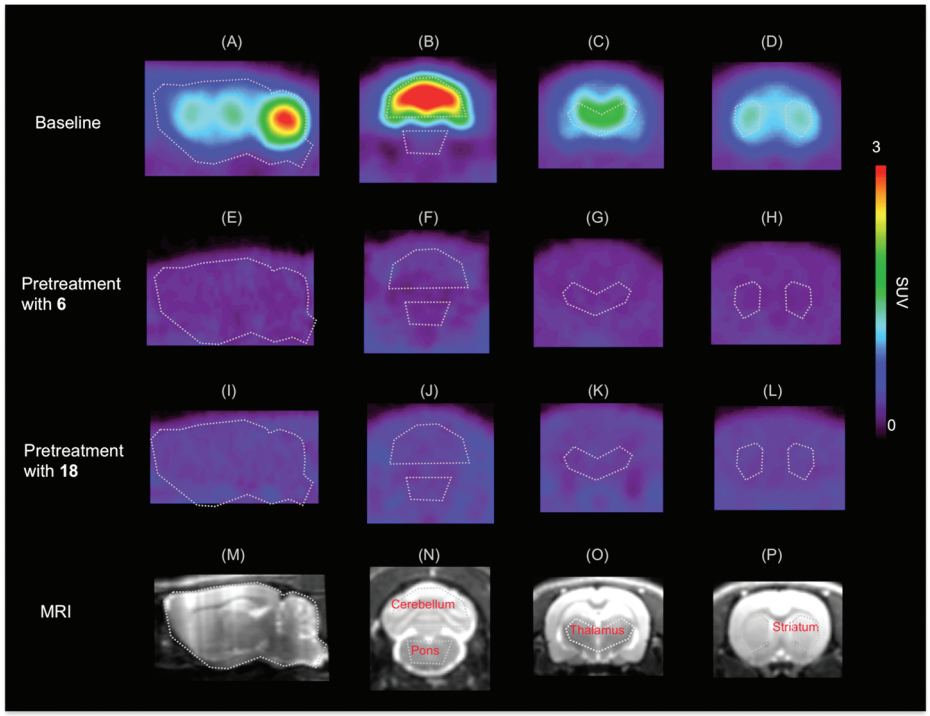

Figure 2. Representative PET and MRI images of isoflurane-anesthetized rat brains. PET images (A–L) were generated by summing the whole scan (0–90 min). Brain regions were confirmed by MRI images of anatomical templates (M–P). (A,E,I,M) sagittal images; left numbers, coronal images. (A–D) [^{11}C]**6** (16 MBq, 0.15 nmol) only; (E–H) [^{11}C]**6** (17 MBq, 0.18 nmol) after treatment with **6** (1 mg/kg); (I–L) [^{11}C]**6** (17 MBq, 0.18 nmol) after treatment with **18** (1 mg/kg).

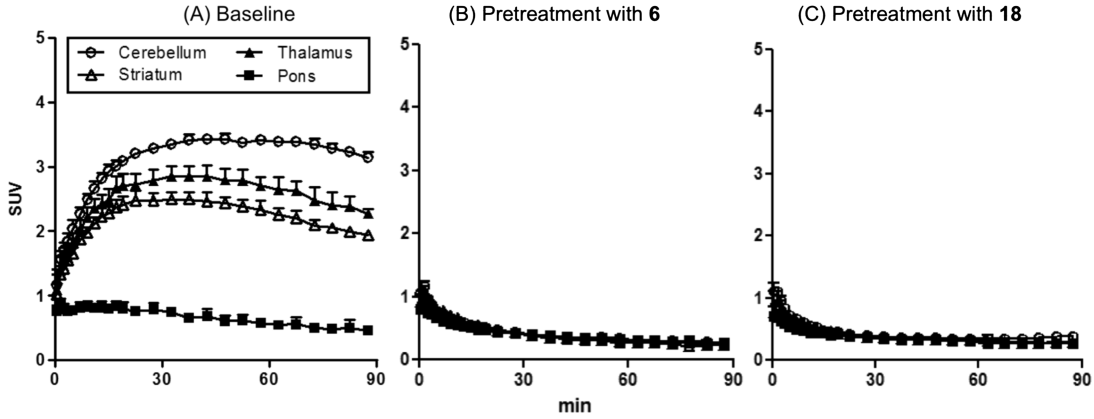

Figure 3. Time–activity curves of PET with [^{11}C]**6** in the cerebellum (circles), thalamus (buried triangles), striatum (blank triangles), and pons (buried squares) of rat brains. (A) [^{11}C]**6** only; (B) [^{11}C]**6** after treatment with **6** (1 mg/kg); (C) [^{11}C]**6** after treatment with **18** (1 mg/kg). Data are the means ± SE.

90% of the maximum at 90 min. Radioactivity in the thalamus and striatum peaked at 45 min and declined slowly to about 80% of the maximum in the corresponding regions until the end of the PET scan. Using the mGluR1-negligible pons as a reference region, the uptake ratio between each region and pons was calculated to reflect in vivo specific binding in the brain. The maximum ratio (n = 4) of each region to the pons was 6.98 ± 1.04 for the cerebellum, 5.05 ± 0.62 for the thalamus, and 4.32 ± 0.21 for the striatum after injection of [^{11}C]**6**.

As shown on the PET images (Figures 2E–H) and TACs (Figure 3B), pretreatment with unlabeled **6** (1 mg/kg) markedly reduced the uptake compared to the control. Uptake was significantly inhibited in all brain regions, and the distribution of radioactivity became fairly uniform throughout the brain. Radioactivity in the cerebellum was reduced to about 15% of the control at 45 min after the injection. The maximum reduction in uptake exceeded 85% in the thalamus and striatum. Pretreatment with mGluR1-selctive **18** also showed significant inhibition of the uptake in regions to a level close to that in the pons and almost abolished the difference in radioactivity among all brain regions (Figures 2I–L and 3C). Such differences in TACs between control (Figure 3A) and **6** or **18**-treated (parts B or C of Figure 3) groups imply the presence of a high proportion of specific binding to mGluR1 in the brain, demonstrating that PET with [^{11}C]**6** could provide significant signals of mGluR1 in brain regions, such as the cerebellum, thalamus, and striatum.

dx.doi.org/10.1021/jm201590g | J. Med. Chem. 2012, 55, 2342–2352

Comparison between Wild-Type and MGluR1 Knockout Mice. PET scan with [^{11}C]**6** was further performed in mGluR1 knockout mice. Figure 4 shows PET images of wild type (Figure 4A) and mGluR1 knockout (Figure 4B) mice. These images showed a significant contrast in brain uptake and distribution. In the wild-type mouse, high brain penetration and accumulation of radioactivity was seen in the cerebellum and thalamus, which was similar to PET images of rat brains and expected for specific binding to mGluR1. In the mGluR1 knockout mouse, only a very low and uniform distribution of radioactivity was determined in the brain. As calculated from the TACs (Supporting Information Figure 4), the values of area under TACs between 0 and 60 min ($AUC_{0-60\ min}$ = SUV × min) were 104 and 100 for the cerebellum and thalamus of wild-type mice, whereas the value was 24 for the whole brain of mGluR1 kockout mice. This difference further demonstrated the specificity for the binding to mGluR1 visualized in the brain after injection of [^{11}C]**6**.

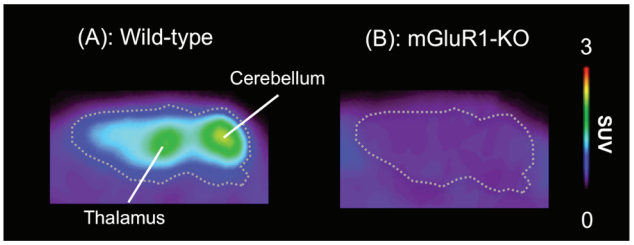

Figure 4. Representative sagittal PET images of wild-type (A) and mGluR1 knockout (B) mouse brains acquired between 0 and 60 min after injection of [^{11}C]**6** (17 MBq, 0.15 nmol).

The present results indicate that [^{11}C]**6** is a promising PET ligand for the imaging of brain mGluR1. Compared to the radioligands listed in Scheme 1, PET with [^{11}C]**6** showed high in vivo specific binding for mGluR1, not only in the cerebellum but also in the thalamus, striatum, etc., of the rat brain. [^{11}C]**6** had improved kinetics over [^{18}F]**5**. After injection of [^{18}F]**5** into rats, the uptake of radioactivity increased during the 90 min PET scan,[21] while at 45 min after the injection of [^{11}C]**6**, uptake peaked and thereafter decreased in the brain slowly. The difference may be related to the decreased binding affinity of [^{11}C]**6** (K_i = 12.6 nM) with mGluR1, in comparison with [^{18}F]**5** (K_i = 5.4 nM). Further, metabolite analysis of rats showed that higher than 80% of total radioactivity in the brain homogenate was due to unchanged [^{11}C]**6** at 90 min after the injection, although its rapid metabolism was determined in the plasma. This suggested that the radiolabeled metabolite of [^{11}C]**6** in the blood could not enter the brain easily, at least not to any large extent and, consequently, the radiolabeled metabolite does not contribute to the nonspecific binding of [^{11}C]**6** in the brain. Detailed comparison of metabolite analysis will be performed between [^{11}C]**6** and [^{18}F]**5** and will be reported elsewhere.

SUMMARY

To visualize brain mGluR1 with PET, three novel ligands **6**–**8** were designed and labeled with ^{11}C or ^{18}F. Of them, **6** showed high in vitro binding affinity for mGluR1 and suitable lipophilicity. This compound was easily labeled with [^{11}C]MeI to give [^{11}C]**6** of two levels of specific activity in a short synthesis time. PET with [^{11}C]**6** of 4370–7840 GBq/μmol is expected to be used to elucidate mGluR1 in mGluR1-low regions, such as the striatum, hippocampus, and cerebral cortex. This study demonstrated that the present pharmacophore is suitable for the development of prospective mGluR1 PET ligands, of which [^{11}C]**6** is promising for evaluation of primate subjects and has further usefulness for the human brain.

EXPERIMENTAL SECTION

1. Materials and Methods. Melting points were measured using a micro melting point apparatus (MP-500P, Yanaco, Tokyo, Japan) and are uncorrected. ^{1}H NMR (300 MHz) spectra were recorded on a JEOL-AL-300 spectrometer (JEOL, Tokyo) with tetramethylsilane as an internal standard. All chemical shifts (δ) were reported in parts per million (ppm) downfield relative to the chemical shift of tetramethylsilane. Signals are quoted as s (singlet), d (doublet), dt (double triplet), t (triplet), q (quartet), br (broad), or m (multiplet). Fast atom bombardment mass spectra (FAB–MS) and high-resolution mass spectra (HRMS) were obtained on a JEOL-AL-300 spectrometer (JEOL) and recorded on the spectrometer. Column chromatography was performed using Wako gel C-200 (70–230 mesh). HPLC was performed using the JASCO HPLC system (JASCO, Tokyo) and Capcell Pack C_{18} columns (Shiseido, Tokyo): 4.6 mm ID × 250 mm for analysis and 10 mm ID × 250 mm for semipreparative purification. Chemical purity of **12** and unlabeled **6**–**8** was analyzed under the following conditions: flow rate, 1.0 mL/min; acetonitrile (MeCN)/H_2O/triethylamine (Et_3N), 6/4/0.01 (v/v/v). Radiochemical purity of [^{11}C]**6**, [^{18}F]**7**, and [^{18}F]**8** was assayed by analytical HPLC with a detector for monitoring radioactivity according to the following conditions: 1.0 mL/min, MeCN/H_2O/Et_3N (6/4/0.01, v/v/v) for [^{11}C]**6** and [^{18}F]**7**; 1.0 mL/min, MeCN/H_2O/Et_3N (6.5/3.5/0.01, v/v/v) for [^{18}F]**8**. Identity of three radioligands was confirmed with the corresponding unlabeled **6**–**8** by HPLC. Under radio-HPLC purification and analysis, effluent radioactivity was monitored using a NaI (Tl) scintillation detector system. All chemical reagents and solvents were purchased from commercial sources (Sigma-Aldrich, MO; Wako Pure Chemical Industries, Osaka, Japan; Tokyo Chemical Industries, Tokyo) and used as supplied. Compound **18** (JNJ-16259685) was purchased from Alexis Biochemicals (San Diego, CA).

Carbon-11 (^{11}C) and fluorine-18 (^{18}F) were produced by ^{14}N (p,α) ^{11}C and ^{18}O (p,n) ^{18}F nuclear reactions using CYPRIS HM-18 cyclotron (Sumitomo Heavy Industry, Tokyo). If not otherwise stated, radioactivity was measured with an IGC-3R Curiemeter (Aloka, Tokyo). For in vitro binding assay [^{18}F]**5** and [^{11}C]**17** were prepared according to the procedures described previously.[20,33]

2. Chemistry. *4-Chloro-6-(1-ethoxyvinyl)pyrimidine (**9**).* A mixture of 4,6-dichloropyrimidine (1.49 g, 10.0 mmol), ethyl 1-(tributylstannyl)vinyl ether (3.4 mL, 10.0 mmol), $Pd(PPh_3)_4$ (348 mg, 0.3 mmol), cesium fluoride (3.04 g, 20 mmol), and copper(I) iodide (190 mg, 1.0 mmol) in *N*,*N*-dimethylformamide (DMF, 30 mL) was stirred at 80 °C for 5 h under N_2 atmosphere. The reaction mixture was quenched with CH_2Cl_2/H_2O (1/1, v/v), and the suspension was filtered through Celite with CH_2Cl_2. The organic layer was washed with water, dried over Na_2SO_4, and evaporated under reduced pressure. The residue was purified by silica gel column chromatography using *n*-hexane/ethyl acetate (15/1, v/v) to give **9** (1.47 g, 63.8% yield) as a colorless solid; mp: 35–37 °C. ^{1}H NMR ($CDCl_3$, δ): 1.45 (3H, t, J = 7.0 Hz), 3.98 (2H, q, J = 7.0 Hz), 4.58 (1H, d, J = 2.2 Hz), 5.71 (1H, d, J = 2.2 Hz), 7.66 (1H, s), 8.89 (1H, s). FAB–MS: m/z 185 (M + H).

*4-(6-Chloropyrimidin-4-yl)-N-methylthiazol-2-amine (**10**).* To a solution of **9** (1.47 g, 8.0 mmol) in THF/H_2O (25 mL; 1/1, v/v) was added 1-bromopyrrolidine-2,5-dione (1.56 g, 8.8 mmol) at room temperature and stirred for 2 h. Methylthiourea (718 mg, 8.0 mmol) was added to the reaction mixture and the mixture was stirred at room temperature for 2 h. The reaction mixture was diluted with water and the resulting solid was filtered and recrystallized from hot THF/water to give **10** (1.11 g, 61.3% yield) as a colorless solid; mp: 190–191 °C. ^{1}H NMR ($CDCl_3$, δ): 3.06 (3H, d, J = 5.1 Hz), 5.20 (1H, br), 7.61 (1H, s), 7.92 (1H, s), 8.89 (1H, s). FAB–MS: m/z 227 (M + H).

*N-[4-(6-Chloropyrimidin-4-yl)-1,3-thiazol-2-yl]-4-methoxy-N-methylbenzamide (**11**).* To a solution of **10** (227 mg, 1.0 mmol) and Et_3N (607 mg, 6.0 mmol) in toluene (5 mL) was added 4-methoxybenzoyl chloride (256 mg, 1.5 mmol) at room temperature under N_2 atmosphere. The reaction mixture was heated at 100 °C for 10 h. This mixture was quenched with water and extracted with CH_2Cl_2. The organic layer was dried over Na_2SO_4 and evaporated under reduced pressure. The residue was purified by silica gel column chromatography using CH_2Cl_2/Et_3N (1/0.001, v/v) and then CH_2Cl_2/ethyl acetate/Et_3N (4/1/0.005, v/v/v) to give **11** (251 mg, 69.6% yield) as a colorless solid; mp: 176−178 °C. ^{1}H NMR ($CDCl_3$, δ): 3.80 (3H, s), 3.89 (3H, s), 7.02 (2H, d, J = 8.8 Hz), 7.60 (2H, d, J = 8.8 Hz), 8.06 (1H, s), 8.10 (1H, s), 8.95 (1H, s). FAB−MS: m/z 361 (M + H).

*N-[4-[6-(Isopropylamino)pyrimidin-4-yl]-1,3-thiazol-2-yl]-4-methoxy-N-methylbenzamide (**6**).* To a solution of **11** (250 mg, 0.7 mmol) and K_2CO_3 (193 mg, 1.4 mmol) in 1,4-dioxane (7 mL) was added isopropylamine (1 mL, 11.7 mmol) at room temperature. The reaction mixture was heated at 80 °C for 16 h. This mixture was quenched with water and extracted with ethyl acetate. The organic layer was washed with brine, dried over Na_2SO_4, and evaporated under reduced pressure. The residue was purified by silica gel column chromatography using *n*-hexane/ethyl acetate/Et_3N (1/4/0.005, v/v/v) to give **6** (191 mg, 71.2% yield) as a colorless solid; mp: 186−188 °C. ^{1}H NMR ($CDCl_3$, δ): 1.29 (6H, d, J = 6.2 Hz), 3.78 (3H, s), 3.88 (3H, s), 4.12 (1H, br), 4.85 (1H, br), 7.00 (2H, d, J = 8.8 Hz), 7.06 (1H, s), 7.59 (2H, d, J = 8.8 Hz), 7.90 (1H, s), 8.57 (1H, s). HRMS (FAB) calcd for $C_{19}H_{22}O_2N_5S$, 384.1494; found, 384.1451.

*4-Hydroxy-N-[4-[6-(isopropylamino)pyrimidin-4-yl]-1,3-thiazol-2-yl]-N-methylbenzamide (**12**).* BBr_3 in dry CH_2Cl_2 (8.3 mL, 1.0 M; 8.3 mmol) was added dropwise to a solution of **6** (640 mg, 1.66 mmol) in dry CH_2Cl_2 (20 mL) at −40 °C under N_2 atmosphere. The reaction mixture was stirred at −40 °C for 1 h and then at room temperature overnight. This mixture was quenched with 2% aqueous Na_2CO_3 solution and extracted with CH_2Cl_2. The organic layer was washed with brine, dried over Na_2SO_4, and evaporated under reduced pressure. The residue was purified by silica gel column chromatography using *n*-hexane/ethyl acetate/Et_3N (1/2/0.003, v/v/v) and then ethyl acetate/methanol/Et_3N (4/1/0.005, v/v/v) to give **12** (185 mg, 30.2% yield) as a colorless solid; mp: 227−229 °C. ^{1}H NMR (DMSO-d_6, δ): 1.16 (6H, d, J = 6.2 Hz), 3.68 (3H, s), 4.12 (1H, br), 6.89 (2H, d, J = 8.1 Hz), 7.10 (1H, s), 7.45 (1H, d, J = 7.0 Hz), 7.57 (2H, d, J = 8.4 Hz), 7.92 (1H, s), 8.41 (1H, s), 10.21 (1H, br). HRMS (FAB) calcd for $C_{18}H_{20}O_2N_5S$, 370.1338; found, 370.1379.

*2-Fluoroethyl 4-Methylbenzenesulfonate (**13**).* To a solution of 2-fluoroethanol (192 mg, 3.0 mmol) and pyridine (480 μL, 6.0 mmol) in dry CH_2Cl_2 (5 mL) was added 4-methylbenzenesulfonyl chloride (629 mg, 3.3 mmol) at 0 °C. The reaction mixture was stirred for 24 h at room temperature. This mixture was quenched with water and extracted with CH_2Cl_2. The organic layer was washed with brine, dried over Na_2SO_4, and evaporated under reduced pressure. The residue was purified by silica gel column chromatography using *n*-hexane/ethyl acetate (3/1, v/v) to give **13** (428 mg, 65.4% yield) as a colorless oil. ^{1}H NMR ($CDCl_3$, δ): 2.46 (3H, s), 4.27 (2H, dt, J = 4.0, 27.1 Hz), 4.58 (2H, dt, J = 4.1, 47.1 Hz), 7.36 (2H, d, J = 8.4 Hz), 7.82 (2H, d, J = 8.4 Hz).

*3-Fluoropropyl 4-Methylbenzenesulfonate (**14**).* To a solution of 3-fluoropropanol (781 mg, 10.0 mmol) and pyridine (1.6 mL, 20.0 mmol) in dry CH_2Cl_2 (15 mL) was added 4-methylbenzenesulfonyl chloride (2.1 g, 11 mmol) at 0 °C. The reaction mixture was stirred for 24 h at room temperature. This mixture was treated as described for **13**. Purification by silica gel column chromatography using *n*-hexane/ethyl acetate (5/1, v/v) gave **14** (1.67 g, 72.0% yield) as a colorless oil. ^{1}H NMR ($CDCl_3$, δ): 1.96−2.12 (2H, m), 2.46 (3H, s), 4.16 (2H, t, J = 6.2 Hz), 4.49 (2H, dt, J = 5.7, 46.9 Hz), 7.36 (2H, d, J = 8.1 Hz), 7.80 (2H, d, J = 8.1 Hz).

*4-Fluoroethoxy-N-[4-[6-(isopropylamino)pyrimidin-4-yl]-1,3-thiazol-2-yl]-N-methylbenzamide (**7**).* To a solution of **12** (100 mg, 0.27 mmol) and K_2CO_3 (57 mg, 0.41 mmol) in anhydrous DMF (5 mL) was added **13** (65 mg, 0.30 mmol). The reaction mixture was stirred for 6 h at 70 °C. This mixture was quenched with water and extracted with ethyl acetate. The organic layer was washed with brine, dried over Na_2SO_4, and evaporated under reduced pressure. The residue was purified by silica gel column chromatography using *n*-hexane/ethyl acetate/Et_3N (1/2/0.003, v/v/v) to give **7** (58 mg, 52.0% yield) as a colorless solid; mp: 172−174 °C. ^{1}H NMR ($CDCl_3$, δ): 1.29 (6H, d, J = 6.2 Hz), 3.77 (3H, s), 4.11 (1H, br), 4.30 (2H, dt, J = 4.2, 27.9 Hz), 4.80 (2H, dt, J = 4.0, 47.3 Hz), 4.82 (1H, br), 7.03 (2H, d, J = 8.8 Hz), 7.06 (1H, s), 7.59 (2H, d, J = 8.8 Hz), 7.90 (1H, s), 8.57 (1H, s). HRMS (FAB) calcd for $C_{20}H_{23}O_2N_5FS$, 416.1557; found, 416.1540.

*4-Fluoropropoxy-N-[4-[6-(isopropylamino)pyrimidin-4-yl]-1,3-thiazol-2-yl]-N-methylbenzamide (**8**).* To a solution of **12** (100 mg, 0.27 mmol) and K_2CO_3 (57 mg, 0.41 mmol) in anhydrous DMF (5 mL) was added **14** (70 mg, 0.30 mmol). The reaction mixture was stirred for 6 h at 70 °C. This mixture was quenched with water and extracted with ethyl acetate. The organic layer was washed with brine, dried over Na_2SO_4, and evaporated under reduced pressure. The residue was purified by silica gel column chromatography using *n*-hexane/ethyl acetate/Et_3N (1/1/0.002, v/v/v) to give **8** (70 mg, 60.4% yield) as a colorless solid; mp: 162−164 °C. ^{1}H NMR ($CDCl_3$, δ): 1.29 (6H, d, J = 6.2 Hz), 2.14−2.30 (2H, m), 3.78 (3H, s), 4.14 (1H, br), 4.18 (2H, t, J = 6.0 Hz), 4.68 (2H, dt, J = 5.7, 47.3 Hz), 4.85 (1H, br), 7.00 (2H, d, J = 6.6 Hz), 7.06 (1H, s), 7.58 (2H, d, J = 6.6 Hz), 7.90 (1H, s), 8.57 (1H, s). HRMS (FAB) calcd for $C_{21}H_{25}O_2N_5FS$, 430.1713; found, 430.1679.

3. Radiochemistry. *N-(4-(6-(Isopropylamino)pyrimidin-4-yl)-1,3-thiazol-2-yl)-4-[^{11}C]methoxy-N-methylbenzamide ([^{11}C]**6**). For Conventional Specific Activity.* [^{11}C]MeI with conventional specific activity was synthesized from cyclotron-produced [^{11}C]CO_2 as described previously.[22] Briefly, [^{11}C]CO_2 was bubbled into 0.04 M $LiAlH_4$ in anhydrous tetrahydrofuran (THF, 300 μL). After evaporation of THF, the remaining complex was treated with 57% hydroiodic acid (300 μL) to give [^{11}C]MeI, which was distilled at 180 °C and transferred by helium gas into a solution of **12** (1.0 mg) and NaOH (5 μL, 0.5 M) in anhydrous DMF (300 μL) at −15 to −20 °C. After radioactivity reached a plateau, this reaction mixture was heated at 70 °C for 5 min. The reaction mixture was applied to the semipreparative HPLC system. HPLC purification was completed using the mobile phase of MeCN/H_2O/Et_3N (6/4/0.01, v/v/v) at a flow rate of 5.0 mL/min. The radioactive fraction corresponding to the desired product was collected in a sterile flask, evaporated to dryness in vacuo, redissolved in 3 mL of sterile normal saline, and passed through a 0.22 μm Millipore filter to give 2.1 GBq of [^{11}C]**6**. The t_R of [^{11}C]**6** was 7.1 min for purification and 6.2 min for analysis on HPLC. Synthesis time from EOB, 25 min; radiochemical yield (decay-corrected), 25% based on [^{11}C]CO_2; radiochemical purity, > 99%; specific activity at EOS, 140 GBq/μmol.

For High Specific Activity. [^{11}C]MeI with high specific activity was synthesized from cyclotron-produced [^{11}C]CH_4 as described previously.[23] Briefly, prior to real production, target gas was irradiated at 20 μA for 5 min and then purged. After the irradiation had been repeated three times, fresh target gas was irradiated at 20 μA for 30 min. The resulting [^{11}C]CH_4 was recovered from the target, concentrated on a Porapak Q trap, passed through a quartz tube kept at 50 °C (I_2 part) and 630 °C (empty part) by helium gas (50 mL/min), and converted to [^{11}C]MeI. Passed through an Ascarite and phosphorus pentoxide column, [^{11}C]MeI was purified and collected in a solution of **12** (1.0 mg) and NaOH (5 μL, 0.5 M) in anhydrous DMF (300 μL) at −15 to −20 °C. After radioactivity reached a plateau, this mixture was warmed to 70 °C and maintained for 5 min. This reaction mixture was treated as described for conventional specific activity to give 1.1 GBq of [^{11}C]**6**. Synthesis time from EOB, 29 min; radiochemical yield (decay-corrected), 6% based on [^{11}C]CH_4; radiochemical purity, >99%; specific activity at EOS, 7840 GBq/μmol.

*4-[^{18}F]Fluoroethoxy-N-[4-[6-(isopropylamino)pyrimidin-4-yl]-1,3-thiazol-2-yl]-N-methylbenzamide ([^{18}F]**7**).* $H_2{}^{18}O$ (95 atom%) was used for irradiation. [^{18}F]HF was recovered from the target, separated from [^{18}O]H_2O, and concentrated on a QMA short column. After

dx.doi.org/10.1021/jm201590g | J. Med. Chem. 2012, 55, 2342−2352

elution from the column with 400 μL of a solution containing aqueous K_2CO_3 (110 mg/8 mL), Kryptofix (330 mg), and MeCN (8 mL), the aqueous [^{18}F]KF was transferred into a reaction vial and evaporated to remove H_2O and MeCN at 110 °C for 15 min. After **15** (7 μL) in 1,2-dichlorobenzene (150 μL) was added to the vial, the reaction mixture was heated at 130 °C to give [^{18}F]FEtBr, which was distilled at once by helium gas (10 mL/min) for 2 min. With the helium flow, [^{18}F]FEtBr was trapped in a solution of **12** (1.0 mg) and NaOH (5 μL, 0.5 M) in anhydrous DMF (300 μL) at −15 to −20 °C. After radioactivity reached plateau, the reaction mixture was heated at 90 °C for 10 min. HPLC purification was completed using a mobile phase of MeCN/H_2O/Et_3N (5.5/4.5/0.01, v/v/v) at a flow rate of 5.0 mL/min. The radioactive fraction corresponding to the desired product was collected in a sterile flask, evaporated to dryness in vacuo, redissolved in 3 mL of sterile normal saline, and passed through a 0.22 μm Millipore filter to give 1.0 GBq of [^{18}F]**7**. The t_R of [^{18}F]**7** was 8.2 min for purification and 6.0 min for analysis on HPLC. Synthesis time, 59 min from EOB; radiochemical yield (decay corrected), 25% based on [^{18}F]F^-; radiochemical purity, >99%; specific activity at EOS, 400 GBq/μmol.

*4-[^{18}F]Fluoropropoxy-N-[4-[6-(isopropylamino)pyrimidin-4-yl]-1,3-thiazol-2-yl]-N-methylbenzamide ([^{18}F]**8**).* To a vial containing dried [^{18}F]KF was added **16** (10 μL) in 1,2-dichlorobenzene (150 μL). The reaction mixture was heated at 180 °C for 2 min to produce [^{18}F]FPrBr, which was distilled by helium gas and trapped into a solution of **12** (1.0 mg) and NaOH (5 μL, 0.5 M) in anhydrous DMF (300 μL) at −15 to −20 °C. After trapping was complete, the reaction mixture was heated at 120 °C for 10 min. HPLC purification was completed using a mobile phase of MeCN/H_2O/Et_3N (5.5/4.5/0.01, v/v/v) at a flow rate of 5.0 mL/min to give 55 MBq of [^{18}F]**8**. The t_R of [^{18}F]**8** was 12.1 min for purification and 6.2 min for analysis on HPLC. Synthesis time from EOB, 58 min; radiochemical yield (decay-corrected), 2% based on total [^{18}F]F^-; radiochemical purity, >99%; specific activity at EOS, 410 GBq/μmol.

4. Measurement and Computation of Lipophilicity. The LogD values were measured by mixing [^{11}C]**6**, [^{18}F]**7**, or [^{18}F]**8** (radiochemical purity: 100%; about 200000 cpm) with *n*-octanol (3.0 g) and sodium phosphate buffer (PBS; 3.0 g, 0.1 M, pH 7.4) in a test tube. The tube was vortexed for 3 min at room temperature, followed by centrifugation at 2330*g* for 5 min. An aliquot of 1 mL of PBS and 1 mL of *n*-octanol was removed, weighted, and counted, respectively. Each samples from the remaining organic layer was removed and repartitioned until consistent LogD value was obtained. The LogD value was calculated by comparing the ratio of cpm/g of *n*-octanol to that of PBS and expressed as LogD = Log[cpm/g (*n*-octanol)/cpm/g (PBS)]. All measurements were performed in triplicate. Meanwhile, the values of cLogD of three radioligands were computed using Pallas 3.4 software (CompuDrug, Sedona, AZ).

5. Animal. DdY mice (male; 8 weeks old; 34−36 g), c57BL/6j mouse (male; 11 weeks old; 24 g), and Sprague−Dawley rats (male; 7−8 weeks old; 210−280 g) were purchased from Japan SLC (Shizuoka, Japan). MGluR1 knockout mouse (male; 12 weeks old; 34 g) was supplied by RIKEN Bioresource Center (Tsukuba, Japan). These animals were housed under a 12 h dark−light cycle and were allowed free access to food pellets and water. The animal experiments were approved by the Animal Ethics Committee of the National Institute of Radiological Sciences.

6. In Vitro Binding Assays. Rats (n = 5) were sacrificed by decapitation under ether anesthesia. The whole brains were rapidly removed and homogenized in 10 volumes of 50 mM Tris-HCl (pH = 7.4) containing 120 mM NaCl with a SilentCrusher S homogenizer (Heidolph Instruments, Schwabach, Germany). The homogenate was centrifuged in polypropylene tube at 40000*g* for 15 min at 4 °C using Optima-TLX (Beckman Coulter, Brea, CA). After the supernatant was discarded, the pellet was resuspended, homogenized, and centrifuged in the same buffer. This procedure was repeated twice to obtain a final pellet of brain homogenate stored at −80 °C before use.

The brain homogenate was diluted to 100 mg/mL in 50 mM Tris-HCl buffer containing 120 mM NaCl, 2 mM KCl, 1 mM $MgCl_2$, and 1 mM $CaCl_2$. Each preparation of 100 μL of homogenate was incubated with [^{18}F]**5** (3 nM in PBS) and 100 μL of tested compounds **5**−**8** (10^{-6} to 10^{-10} M in 0.1% dimethylsulfoxide) in a final volume of 1.0 mL buffer, respectively. These mixtures were incubated for 1 h at room temperature. The bound and free radioactivity were separated by vacuum filtration through 0.3% polyethylenimine-pretreated Whatman GF/C glass fiber filters using a cell harvester (M-24, Brandel, Gaithersburg, MD), followed by washing with prechilled buffer three times. The filters containing the bound [^{18}F]**5** were assayed for radioactivity by a 1480 Wizard autogamma scintillation counter (Perkin-Elmer, Waltham, MA). In the present study, the dissociation constant (K_d) of [^{18}F]**5** for mGluR1 in the brain homogenate was determined by using the Scatchard analysis. Subsequently, we performed the same assay with [^{11}C]**17**, an antagonistic radioligand for mGluR5, as described above. The results of inhibitory experiments were subjected to nonlinear regression analysis using Prism 5 (GraphPad Software, La Jolla, CA) by which IC_{50} and the inhibition constant (K_i) values were calculated.

7. In Vitro Autoradiography. Rat brain sections (20 μm) were preincubated for 20 min in 50 mM Tris-HCl buffer (pH 7.4) containing 1.2 mM $MgCl_2$ and 2 mM $CaCl_2$ at room temperature. After preincubation, these sections were incubated for 30 min at room temperature in the fresh buffer containing [^{11}C]**6** (9.2 MBq, 0.5 nM), [^{18}F]**7** (0.4 MBq, 5 pM), or [^{18}F]**8** (0.4 MBq, 4 pM). Compound **18** (1 μM) were used to determine the specific binding of these radioligands for mGluR1. After incubation, these brain sections were washed (3 × 5 min) with cold buffer, dipped in cold distilled water, and dried with cold air. These sections were placed on contact with imaging plates (BAS-MS2025, FUJIFILM, Tokyo). Autoradiograms were obtained and photostimulated luminescence values (PSL) in the regions of interest were measured using a Bio-Imaging Analyzer System (BAS5000, FUJIFILM).

8. Biodistribution Study in Mice. A saline solution of [^{11}C]**6** (4.8 MBq/140 μL, 40 pmol) was injected into mice via the tail vein. Four mice were sacrificed at 1, 5, 15, 30, and 60 min after the injection by cervical dislocation, respectively. The whole brain, heart, liver, lung, spleen, testis, kidney, small intestine (including contents), muscle, and blood samples were quickly removed. Radioactivity present in these tissues was measured with an autogamma counter (1480 Wizard) and expressed as the percentage of injected dose per gram of wet tissue (% ID/g). All radioactivity measurements were decay-corrected.

9. Small-Animal PET Studies. *For Normal Rats.* Prior to PET scans, anatomical template images of rat brain were generated by a high-resolution magnetic resonance imaging (MRI) system.[35] Briefly, a rat was anesthetized with sodium pentobarbital (50 mg/kg, ip), and scanned with a 400 mm bore, 7 T horizontal magnet (NIRS/KOBELCO, Kobe, Japan/Bruker BioSpin, Ettlingen, Germany) equipped with 120 mm diameter gradients (Bruker BioSpin). A 72 mm diameter coil was used for radiofrequency transmission, and signals were received by a 4-channel surface coil. Coronal T2-weighted MRI images were obtained by a fast spin−echo sequence with the following imaging parameters: repetition time = 8000 ms, effective echo time = 15 ms, field of view = 35 mm ×35 mm, and slice thickness = 0.6 mm.

A rat was placed in a small-animal PET scanner (Siemens Medical Solutions, Knoxville, TN). Body temperature was maintained with a 40 °C water circulation system (T/Pump TP401, Gaymar Industries, Orchard Park, NY). The rat was kept under anesthesia with 1.5% (v/v) isoflurane during the scan. To inject [^{11}C]**6**, a 24-gauge needle with catheter (Terumo Medical Products, Tokyo) was placed into the rat tail vein. A dynamic emission scan in 3D list mode was performed for 90 min (1 min ×4 scans, 2 min ×8 scans, 5 min ×14 scans). For inhibitory study, unlabeled **6** (1 mg/kg) or **18** (3 mg/kg) was injected via the tail vein catheter just before a bolus injection of [^{11}C]**6** (37−55 MBq/100 μL, 0.3−0.5 nmol). PET dynamic images were reconstructed with filtered back-projection using a Hanning's filter, a Nyquist cutoff of 0.5 cycle/pixel.

For Mice. A wild-type or mGluR1 knockout mouse was secured in a custom-designed chamber, placed in the Inveon PET scanner, and prepared as described above. A 29-gauge needle with 12−15 cm of

polyethylene 10 tube prepared in-house was placed into the tail vein of mouse to inject [^{11}C]**6** (5 MBq/100 μL, 45 pmol). A dynamic emission scan in 3D list mode was performed for 60 min (1 min ×4 scans, 2 min ×8 scans, 5 min ×8 scans).

Image Acquisition and Data Analysis. The PET images were reconstructed using ASIPro VM software (Analysis Tools and System Setup/Diagnostics Tool, Siemens Medical Solutions) with each PET image by individual experience. Volumes of interest were placed on the striatum, thalamus, pons, and cerebellum using ASIPro VM (Siemens Medical Solutions) with reference to the MRI template. Brain uptake of radioactivity was decay-corrected to the injection time and was expressed as the standardized uptake value (SUV), which was normalized to the injected radioactivity and body weight. SUV = (radioactivity per milliliter tissue/injected radioactivity) × gram body weight.

■ ASSOCIATED CONTENT

Supporting Information

Purities of **6**–**8** and **12** determined by HPLC; HPLC analytic charts for **6**–**8** and **12**; HPLC purification charts for [^{11}C]**6**, [^{18}F]**7**, and [^{18}F]**8**; HPLC analytical charts for [^{11}C]**6**, [^{18}F]**7**, and [^{18}F]**8**; Chemical structures of [^{11}C]**17** and **18**; time–activity curves in the wild-type and mGluR1 knockout mouse brains after injection of [^{11}C]**6**. This material is available free of charge via the Internet at http://pubs.acs.org.

■ AUTHOR INFORMATION

Corresponding Author

*Phone: 81-43-382-3708. Fax: 81-43-206-3261. E-mail: zhang@nirs.go.jp. Address: Department of Molecular Probes, Molecular Imaging Center, National Institute of Radiological Sciences, 4-9-1 Anagawa, Inage-ku, Chiba 263-8555, Japan.

Author Contributions

‖These authors contributed equally.

Notes

The authors declare no competing financial interest.

■ ACKNOWLEDGMENTS

We thank the staff of National Institute of Radiological Sciences for support with the cyclotron operation, radioisotope production, radiosynthesis, and animal experiments. We are also grateful to Dr. Tatsumi Hirata (National Institute of Genetics, Shizuoka, Japan) for development of mGluR1 knockout mouse. This study was supported in part by Grants-in-Aid for Scientific Research (Basic Research C: 22591379) from the Ministry of Education, Culture, Sports, Science and Technology, Japanese Government.

■ ABBREVIATIONS USED

AUC, area under time–activity curve; BBr_3, boron tribromide; [^{11}C]CH_4, [^{11}C]methane; CNS, central nervous system; [^{11}C]CO_2, [^{11}C]carbon dioxide; DMF, *N*,*N*-dimethyl formamide; EOB, end of bombardment; EOS, end of synthesis; Et_3N, triethylamine; FAB-MS, fast atom bombardment mass spectra; [^{18}F]FEtBr, 1-bromo-2-[^{18}F]fluoroethane; [^{18}F]FPrBr, 1-bromo-3-[^{18}F]fluoropropane; HPLC, high-performance liquid chromatography; HRMS, high-resolution mass spectra; %ID/g, percentage of the injected dose per gram of wet tissue; Kryptofix 222, 4,7,13,16,21,24-hexaoxa-1,10-diazabicyclo-[8,8,8]hexacosane; $LiAlH_4$, lithium aluminum hydride; MeCN, acetonitrile; [^{11}C]MeI, [^{11}C]methyl iodide; mGluR1, metabotropic glutamate receptor type 1; mGluR5, metabotropic glutamate receptor type 5; MRI, magnetic resonance imaging; PBS, phosphate buffer solution; $Pd(PPh_3)_4$, tetrakis-(triphenylphosphine)palladium(0); PET, positron emission tomography; SUV, standardized uptake value; TAC, time–activity curve; t_R, retention time

■ REFERENCES

(1) Nakanishi, S. Metabotropic glutamate receptors: synaptic transmission, modulation, and plasticity. *Neuron* **1994**, *13*, 1031–1037.
(2) Conn, P. J.; Pin, J. P. Pharmacology and functions of metabotropic glutamate receptors. *Annu. Rev. Pharmacol. Toxicol.* **1997**, *37*, 205–237.
(3) Bordi, F.; Ugolini, A. Group I metabotropic glutamate receptors: implications for brain diseases. *Prog. Neurobiol.* **1999**, *59*, 55–79.
(4) Ferraguti, F.; Crepaldi, L.; Nicoletti, F. Metabotropic glutamate 1 receptor: current concepts and perspectives. *Pharmacol. Rev.* **2008**, *60*, 536–581.
(5) Kew, J. N. Positive and negative modulation of metabotropic glutamate receptors: emerging therapeutic potential. *Pharmacol. Ther.* **2004**, *104*, 233–244.
(6) Swanson, C. J.; Bures, M.; Johnson, M. P.; Linden, A. M.; Monn, J. A.; Schoepp, D. D. Metabotropic glutamate receptors as novel targets for anxiety and stress disorders. *Nature Rev. Drug Discovery* **2005**, *4*, 131–144.
(7) Schkeryantz, J. M.; Kingston, A. E.; Johnson, M. P. Prospects for metabotropic glutamate 1 receptor antagonists in the treatment of neuropathic pain. *J. Med. Chem.* **2007**, *50*, 2563–2568.
(8) Wu, W. L.; Burnett, D. A.; Domalski, M.; Greenlee, W. J.; Li, C.; Bertorelli, R.; Fredduzzi, S.; Lozza, G.; Veltri, A.; Reggiani, A. Discovery of orally efficacious tetracyclic metabotropic glutamate receptor 1 (mGluR1) antagonists for the treatment of chronic pain. *J. Med. Chem.* **2007**, *50*, 5550–5553.
(9) Suzuki, G.; Kimura, T.; Satow, A.; Kaneko, N.; Fukuda, J.; Hikichi, H.; Sakai, N.; Maehara, S.; Kawagoe-Takaki, H.; Hata, M.; Azuma, T.; Ito, S.; Kawamoto, H.; Ohta, H. Pharmacological characterization of a new, orally active and potent allosteric metabotropic glutamate receptor 1 antagonist, 4-[1-(2-fluoropyridin-3-yl)-5-methyl-1*H*-1,2,3-triazol-4-yl]-*N*-isopropyl-*N*-methyl-3,6-dihydropyridine-1(2*H*)-carboxamide (FTIDC). *J. Pharmacol. Exp. Ther.* **2007**, *32*, 1144–1153.
(10) Kohara, A.; Takahashi, M.; Yatsugi, S.; Tamura, S.; Shitaka, Y.; Hayashibe, S.; Kawabata, S.; Okada, M. Neuroprotective effects of the selective type 1 metabotropic glutamate receptor antagonist YM-202074 in rat stroke models. *Brain Res.* **2008**, *1191*, 168–179.
(11) Fotuhi, M.; Sharp, A. H.; Glatt, C. E.; Hwang, P. M.; von Krosigk, M.; Snyder, S. H.; Dawson, T. M. Differential localization of phosphoinositide-linked metabotropic glutamate receptor (mGluR1) and the inositol 1,4,5-trisphosphate receptor in rat brain. *J. Neurosci.* **1993**, *13*, 2001–2012.
(12) Lavreysen, H.; Pereira, S. N.; Leysen, J. E.; Langlois, X.; Lesage, A. S. Metabotropic glutamate 1 receptor distribution and occupancy in the rat brain: a quantitative autoradiographic study using [^{3}H]-R214127. *Neuropharmacology* **2004**, *46*, 609–619.
(13) Huang, Y.; Narendran, R.; Bischoff, F.; Guo, N.; Zhu, Z.; Bae, S. A.; Lesage, A. S.; Laruelle, M. A positron emission tomography radioligand for the in vivo labeling of metabotropic glutamate 1 receptor: (3-ethyl-2-[^{11}C]methyl-6-quinolinyl) (*cis*-4-methoxycyclohexyl)methanone. *J. Med. Chem.* **2005**, *48*, 5096–5099.
(14) Yanamoto, K.; Konno, F.; Odawara, C.; Yamasaki, T.; Kawamura, K.; Hatori, A.; Yui, J.; Wakizaka, K.; Nengaki, N.; Takei, M.; Zhang, M.-R. Radiosynthesis and evaluation of [^{11}C]YM-202074 as a PET ligand for imaging the metabotropic glutamate receptor type 1. *Nucl. Med. Biol.* **2010**, *37*, 615–624.
(15) Prabhakaran, J.; Majo, V. J.; Milak, M. S.; Kassir, S. A.; Palner, M.; Savenkova, L.; Mali, P.; Arango, V.; Mann, J. J.; Parsey, R. V.; Kumar, J. S. Synthesis, in vitro and in vivo evaluation of [^{11}C]MMTP: a potential PET ligand for mGluR1 receptors. *Bioorg. Med. Chem. Lett.* **2010**, *20*, 3499–3501.
(16) Hostetler, E. D.; Eng, W.; Joshi, A. D.; Sanabria-Bohórquez, S.; Kawamoto, H.; Ito, S.; O'Malley, S.; Krause, S.; Ryan, C.; Patel, S.;

Williams, M.; Riffel, K.; Suzuki, G.; Ozaki, S.; Ohta, H.; Cook, J.; Burns, H. D.; Hargreaves, R. Synthesis, characterization, monkey PET studies of [^{18}F]MK-1312, a PET tracer for quantification of mGluR1 receptor occupancy by MK-5435. *Synapse* **2010**, *65*, 125−135.

(17) Ohgami, M.; Haradahira, T.; Takai, N.; Zhang, M.-R.; Kawamura, K.; Yamasaki, K.; Yanamoto, K. [^{18}F]FTIDC: a New PET radioligand for metabotropic glutamate receptor 1. *Eur. J. Nucl. Med. Mol. Imag.* **2009**, *36* (suppl 2), S310.

(18) Fujinaga, M.; Yamasaki, T.; Kumata, K.; Kawamura, K.; Hatori, A.; Yanamoto, K.; Yui, J.; Yoshida, Y.; Ogawa, M.; Nengaki, N.; Maeda, J.; Fukumura, T.; Zhang, M.-R. Synthesis and evaluation of 6-[1-(2-[^{18}F]fluoro-3-pyridyl)-5-methyl-1*H*-1,2,3-triazol-4-yl]quinoline for positron emission tomography imaging of the metabotropic glutamate receptor type 1 in brain. *Bioorg. Med. Chem.* **2011**, *19*, 102−110.

(19) Fujinaga, M.; Hatori, A.; Maeda, J.; Yamasaki, T.; Yui, J.; Kawamura, K.; Kumata, K.; Yoshida, Y.; Okauchi, T.; Nagai, Y.; Higuchi, M.; Zhang, M.-R. ^{18}F-FPIT: A PET ligand for imaging of the metabotropic glutamate receptor type 1 in rodent and primate brains. *J. Neurochem.* **2011**, DOI: 10.1111/j.1471-4159.2011.07348.x.

(20) Yamasaki, T.; Fujinaga, M.; Yoshida, Y.; Kumata, K.; Yui, J.; Kawamura, K.; Hatori, A.; Fukumura, T.; Zhang, M.-R. Radiosynthesis and preliminary evaluation of 4-[^{18}F]fluoro-*N*-[4-[6-(isopropylamino)-pyrimidin-4-yl]-1,3-thiazol-2-yl]-*N*-methylbenzamide as a new positron emission tomography ligand for metabotropic glutamate receptor subtype 1. *Bioorg. Med. Chem. Lett.* **2011**, *21*, 2998−3001.

(21) Yamasaki, T.; Fujinaga, M.; Maeda, J.; Hatori, A.; Yui, J.; Kawamura, K.; Higuchi, M.; Suhara, T.; Fukumura, T.; Zhang, M.-R. Imaging for metabotropic glutamate receptor subtype 1 in rat and monkey brains using PET with [^{18}F]FITM. *Eur. J. Nucl. Med. Mol. Imaging* **2012**, DOI: 10.1007/s00259-011-1995-6.

(22) Suzuki, K.; Inoue, O.; Hashimoto, K.; Yamasaki, T.; Kuchiki, M.; Tamate, T. Computer-controlled large scale production of high specific activity [^{11}C]Ro15−1788. *Appl. Radiat. Isot.* **1985**, *36*, 971−976.

(23) Noguchi, J.; Suzuki, K. Automated synthesis of the ultra high specific activity of [^{11}C]Ro15−4513 and its application in an extremely low concentration region to an ARG study. *Nucl. Med. Biol.* **2003**, *30*, 335−343.

(24) Satoh, A.; Nagatomi, Y.; Hirata, Y.; Ito, S.; Suzuki, G.; Kimura, T.; Maehara, S.; Hikichi, H.; Satow, A.; Hata, M.; Ohta, H.; Kawamoto, H. Discovery and in vitro and in vivo profiles of 4-fluoro-*N*-[4-[6-(isopropylamino)pyrimidin-4-yl]-1,3-thiazol-2-yl]-*N*-methylbenzamide as a novel class of an orally active metabotropic glutamate receptor 1 (mGluR1) antagonist. *Bioorg. Med. Chem. Lett.* **2009**, *19*, 5464−5468.

(25) Chi, D. Y.; Kilbourn, M. R.; Katzenellenbogen, J. A.; Welch, M. J. A rapid and efficient method for the fluoroalkylation of amines and amides. Development of a method suitable for incorporation of the short-lived positron emitting radionuclide fluorine-18. *J. Org. Chem.* **1987**, *52*, 658−664.

(26) Fukumura, T.; Suzuki, H.; Mukai, K.; Zhang, M.-R.; Yoshida, Y.; Nemoto, K.; Suzuki, K. Development of versatile synthesis equipment for multiple production of PET radiopharmaceuticals. *J. Label. Compd. Radiopharm.* **2007**, *50*, S202.

(27) Noguchi, J.; Zhang, M.-R.; Yanamoto, K.; Suzuki, K. In vitro binding of [^{11}C]raclopride with ultra-high specific activity in rat brain determined by homogenate assay and autoradiography. *Nucl. Med. Biol.* **2008**, *35*, 19−27.

(28) Yui, J.; Hatori, A.; Kawamura, K.; Kawamura, K.; Yanamoto, K.; Yamasaki, T.; Ogawa, M.; Yoshida, Y.; Kumata, K.; Fujinaga, M.; Nengaki, N.; Fukumura, T.; Suzuki, K.; Zhang, M.-R. Visualization of early infarction in rat brain after ischemia using a translocator protein (18 kDa) PET ligand [^{11}C]DAC with ultra-high specific activity. *NeuroImage* **2011**, *54*, 123−130.

(29) Wilson, A. A.; Dasilva, J. N.; Houle, S. Synthesis of two radiofluorinated cocaine analogues using distilled 2-[18F]fluoroethyl bromide. *Appl. Radiat. Isot.* **1995**, *46*, 765−770.

(30) Zhang, M.-R.; Tsuchiyama, A.; Haradahira, T.; Yoshida, Y.; Furutsuka, K.; Suzuki, K. Development of an automated system for synthesizing ^{18}F-labeled compounds using [^{18}F]fluoroethyl bromide as a synthetic precursor. *Appl. Radiat. Isot.* **2002**, *57*, 335−342.

(31) Zhang, M.-R.; Maeda, J.; Ogawa, M.; Noguchi, J.; Ito, T.; Yoshida, Y.; Okauchi, T.; Obayashi, S.; Suhara, T.; Suzuki, K. Development of a new radioligand, *N*-(5-fluoro-2-phenoxyphenyl)-*N*-(2-[^{18}F]fluoroethyl-5-methoxybenzyl)acetamide, for PET imaging of peripheral benzodiazepine receptor in primate brain. *J. Med. Chem.* **2004**, *47*, 2228−2235.

(32) Pike, V. W. PET radiotracers: crossing the blood−brain barrier and surviving metabolism. *Trends Pharmacol. Sci.* **2009**, *30*, 431−440.

(33) Ametamey, S. M.; Kessler, L. J.; Honer, M.; Wyss, M. T.; Buck, A.; Hintermann, S.; Auberson, Y. P.; Gasparini, F.; Schubiger, P. A. Radiosynthesis and preclinical evaluation of 11C-ABP688 as a probe for imaging the metabotropic glutamate receptor subtype 5. *J. Nucl. Med.* **2006**, *47*, 698−705.

(34) Lavreysen, H.; Wouters, R.; Bischoff, F.; Nóbrega Pereira, S.; Langlois, X.; Blokland, S.; Somers, M.; Dillen, L.; Lesage, A. S. JNJ16259685, a highly potent, selective and systemically active mGlu1 receptor antagonist. *Neuropharmacology* **2004**, *47*, 961−972.

(35) Yui, J.; Maeda, J.; Kumata, K.; Kawamura, K.; Yanamoto, K.; Yamasaki, T.; Hatori, A.; Nengaki, N.; Higuchi, M.; Zhang, M.-R. ^{18}F-FEAC and ^{18}F-FEDAC: Monkey PET and imaging of translocator protein (18 kDa) in the brains of infarcted rats. *J. Nucl. Med.* **2010**, *51*, 1301−1309.